iVES OENO One vine & wine

DOI: https://doi.org/10.20870/oeno-one.2026.60.2.9759

OPEN ACCESS



SPECIAL ISSUE

Integrating sensor-based systems for mapping intra-vineyard variability in the Valpolicella area: potential and constraints

Ron Shmuleviz[1,*], Marianna Fasoli[1], Giovanni Battista Tornielli[1,2,3]

[1] Department of Biotechnology, University of Verona, Strada Le Grazie 15, 37134 Verona, Italy
[2] Department of Agronomy, Food, Natural Resources, Animals and Environment, University of Padova, Viale dell'Università 16, 35020 Legnaro (PD), Italy
[3] Interdepartmental Centre for Research in Viticulture and Enology (CIRVE), University of Padova, Via XXVIII Aprile 14, 31015 Conegliano (TV), Italy

This article is an original research article published in cooperation with the International Scientific Congress GreenWINE, May 19–20, 2025, Verona, Italy.

Guest editors: Luca Rolle, Dominik Durner.

Article number: 9759

*correspondence:
ron.shmuleviz@univr.it

Associate editor:
Luca Rolle

Received:
18 November 2025

Accepted:
24 April 2026

Published:
22 May 2026

This article is published under the **Creative Commons licence** (CC BY 4.0).

Use of all or part of the content of this article must mention the authors, the year of publication, the title, the name of the journal, the volume, the pages and the DOI in compliance with the information given above.

ABSTRACT

Precision viticulture methods should be adapted to the viticultural context to provide relevant insights. This study evaluated the potential and constraints of established precision viticulture techniques in the Valpolicella wine region, which is characterised by small, irregularly shaped vineyard parcels trained using the traditional overhead Pergola system, and where mixed plots of autochthonous cultivars are often grown. Two vineyards were monitored for intra-vineyard variability, one of which was assessed over two seasons. Sentinel-2 and UAV-derived parameters were measured along with ground-based sensor data, including the canopy crop water stress index (CWSI), soil volumetric water content (VWC), and NDVI. Traditional agronomic measurements and berry quality parameters were also collected and integrated with sensor data into a dataset, which was then explored using multivariate analysis to validate the sensor data. Despite structural features that were expected to challenge top-down remote sensing, the Sentinel-2 and UAV-derived data exhibited highly similar spatial patterns and were in turn consistent with ground-based measurements. This result may be attributable to the horizontal pergola canopy, which enhanced its visibility from above. In the autochthonous multivarietal vineyard, the sensor-derived data successfully identified intra-parcel variability in agronomic parameters, independently of the cultivar plot layout. Skin thickness, a highly relevant berry trait for Valpolicella wines produced from withered grapes, was negatively correlated with CWSI. This study highlights the value of an integrated multiple-parameter approach that leverages sensor-derived data and paves the way for precision viticulture application in the Valpolicella.

KEYWORDS: intra-parcel variability, NDVI, CWSI, Sentinel-2, GreenWINE 2025, sensors

INTRODUCTION

The application of sensor systems in viticulture allows rapid and comprehensive data collection across extended parcels, enabling the detection of intra-vineyard variability and improvement of vineyard management (Ammoniaci *et al.*, 2021; Ferro & Catania, 2023; Loggenberg *et al.*, 2024; Mizik, 2023).

Despite their widespread use, the precision and accuracy of sensor data are highly sensitive to operational conditions, which strongly depend on the viticultural context. Specific climatic conditions and landscape configurations may increase or decrease the overall spatial variability and affect the regional relevance of precision viticulture (Bramley *et al.*, 2019; Ledderhof *et al.*, 2017). Different vineyard structural features, such as topography, plant density, trellis systems, row orientation, and soil, may influence the interpretation of remote sensing data (Zanchin *et al.*, 2024). Moreover, sensor-derived vigour variability does not always have the same agronomic significance. While high vigour is often associated with delayed ripening and lower quality (Reynolds, 2010), its effect can be limited for intrinsically vigorous cultivars (Squeri *et al.*, 2021) or even be beneficial under warm conditions, as it improves the berry microclimate leading to high berry quality (Bonilla *et al.*, 2015). Therefore, sensor applications in new viticultural scenarios are usually accompanied by preliminary evaluations and adaptations of existing approaches to the specific characteristics of each environment.

The Valpolicella wine region, located in northeastern Italy, is an area where sensor-based approaches have not yet been fully integrated into or adapted to the local viticulture. The shift toward modern mechanised viticulture has resulted in the reconfiguration of Valpolicella's landscape, which was historically dominated by terraced vineyards but is now characterised by levelled vineyard layouts. This results in a high degree of soil variability across the region, as well as small-sized and irregularly shaped vineyards. Despite modernisation, viticulture in Valpolicella remains traditional. Mostly autochthonous varieties (*e.g.*, Corvina, Corvinone, Rondinella, Molinara) are cultivated using the traditional overhead Pergola trellis system, in which grape clusters hang beneath the canopy. The region further maintains an ancient winemaking practice, named *withering*, a postharvest technique employed to produce high-quality, prestigious wines vinified from slowly and partially dehydrated grapes (Accordini, 2013). To ensure slow dehydration kinetics, berry and cluster morphological parameters should be taken into consideration, and harvest is therefore often selective. These structural, varietal, and production-specific features should be evaluated to determine whether meaningful information can be extracted using conventional precision viticulture techniques.

This work aimed to evaluate the informative potential of various sensor systems for detecting intra-parcel variability within two Valpolicella vineyards representative of the region's landscape and agronomic characteristics. Through the integration of remote and ground-based data, the study examined both the strengths and the constraints of applying precision viticulture tools within this regional, environmental, and agronomic context.

MATERIALS AND METHODS

1. Vineyards

1.1. Pedemonte

Vineyard #1 was located in Pedemonte (Verona, north-east Italy; 45°30'25.13" N, 10°55'27.78" E) at 120 m above sea level, covering 0.7 ha and consisting of seven 318 m-long vine rows oriented ~ 20° eastward from the north-south axis. The parcel was divided by a dirt road into two uniformly managed sections. Cv. Corvina 10-year-old vines were grown organically and trained to a Pergola trellis system at a height of 1.5 m, with a row and vine spacing of 3.5 m and 1.0 m, respectively. Vines were pruned to two 10–12 bud fruiting canes. Drip irrigation was supplied by a line installed 40 cm below the cane wire, with emitters spaced 0.5 m that were activated depending on the seasonal weather conditions. This vineyard was monitored across six blocks of 15 vines over two years (2023–2024).

1.2. Nassar

Vineyard #2 was located in Nassar (San Pietro in Cariano, Verona, north-east Italy; 45°29'4.86" N, 10°55'24.94" E) at 83 m above sea level. The 25-year-old vines were non-irrigated and trained to a Pergola trellis system over an area covering 0.9 ha. The row and vine spacing were 4 and 1 m, respectively, with 1.7 m vertical trunks pruned to four 10–12 buds fruiting canes per vine. The rows were oriented ~ 15° westward from the north-south axis, featuring alternating plots of four different cultivars: six rows of Molinara, eight rows of Corvina, nine rows of Corvinone, and nine rows of Rondinella. Eight blocks were selected (two blocks per cultivar plot) and monitored during the 2022 season.

2. Ground-truth measurements

2.1. Vine measurements

In both vineyards, bud fruitfulness was assessed after tendril growth during phenological stages #53–57 using the BBCH scale (Lorenz *et al.*, 1995). Bud fruitfulness was assessed on six randomly selected canes per block, and was calculated as the number of inflorescences (excluding those from secondary shoots) per total number of buds, including undeveloped ones.

In Nassar vineyard, further vine measurements were conducted. Six additional shoots per block were randomly selected and measured for their lengths at three time points during #15–67 BBCH (Lorenz *et al.*, 1995). The weekly increase was divided by seven to calculate daily shoot elongation. Three additional shoots per block were randomly sampled during #67 BBCH (Lorenz *et al.*, 1995), and were used to calculate the leaf area-to-length ratio: individual leaves on each shoot were measured to determine total leaf area using a LI-3100C Area Meter (LI-COR Biosciences, Lincoln, NE, USA), and this value was normalised by the corresponding shoot length. To estimate total leaf area per vine, the average leaf area-to-length ratio was multiplied by the average shoot length at #67 BBCH (Lorenz *et al.*, 1995),

the average number of shoots per cane (comprising the six canes assessed for bud fruitfulness), and four canes per vine in the Nassar trellis system.

At harvest, the yield was determined in both vineyards. Clusters from the primary shoots of three and six vines per block in Nassar and Pedemonte, respectively, were harvested, counted, and weighed to determine the average cluster weight and yield per vine.

2.2. Berry quality parameters

At around #86–88 BBCH (Lorenz *et al.*, 1995), the mid-late stages of berry ripening, a pool of approximately 200 berries was randomly collected from each block. Skin thickness was determined on 30 berries using a digital microcaliper (Hoffmann Group, Padova, Italy) after carefully separating the skins from the pulp and drying them to remove surface moisture. A further 150 berries were divided into three lots and weighed using a digital scale (EU500, Gibertini elettronica srl, Milan, Italy). Next, the berries were crushed and the juice was used to determine total soluble solids (TSS) and pH employing a digital refractometer (HI96811, Hanna Instruments, Padova, Italy) and a pH-meter (HI96812, Hanna Instruments, Padova, Italy), respectively. Titratable acidity (TA) was determined by manual titration of 7 mL of must with 0.1 M NaOH as the titrant. The anthocyanin and polyphenol content were determined by adjusting the method reported in Di Stefano and Cravero (1991). Fresh berry skins of the remaining berries from the same pool were separated from the pulps, and 6 g of skins were macerated in 15 % ethanol, 5 g/L tartaric acid and 100 mg/L metabisulfite for 72 h. The macerates were read in a Cary 50 UV-Visible Spectrophotometer (Varian Inc., Turin, Italy) after being diluted with an ethanolic solution of HCl (70:30:1, ethanol:H_2O:HCl, *v/v*). The reading was carried out at 280 and 540 nm to detect total polyphenol and anthocyanin content, respectively. The absorption results were interpreted by a calibration curve prepared with gallic acid and malvidin-3-O-β glucoside standards and expressed as mg/g.

3. Ground-based sensors

3.1. Vine and soil water status

A handheld thermal camera was used to capture the canopy temperature employing FLIR E6 (320 × 240 pixels; Teledyne FLIR LLC, Wilsonville, Oregon, USA), which was used to calculate the crop water stress index (CWSI) as described in Jones *et al.* (2002). A leaf sprayed with water and imaged five minutes after application was used as the wet reference, while a leaf covered with vaseline and imaged 25 minutes after application served as the dry reference. The reference images were captured at the beginning and end of each sampling and averaged for wet and dry references, respectively. Sampling was conducted during the hottest months of the year, July and August, within an optimal midday window (12:00–14:00) to detect differences in vine water status not associated with severe water stress (Ru *et al.*, 2020).

To access the sun-exposed side of the Pergola canopy, a small ladder was used, with 10 images taken approximately 60 cm from the canopy. Non-canopy pixels (*e.g.*, trellis system wires, dry leaves, sky, soil) were cleaned from each image employing Exiftool (Harvey, 2016) in the R Studio environment (R Core Team, 2021), using the R packages *Thermimage* (Tattersall, 2021).

A FieldScout TDR 350 Soil Moisture Meter (Spectrum Technologies INC., Aurora, IL, USA) was used to measure the soil volumetric water content (VWC) by positioning two 20 cm probes vertically to the ground, in 10 sites within each block, in the vine root zone, and at least 30 cm distant from the emitters. Samplings were scheduled at least two days after any rainfall.

3.2. Canopy vigour

Canopy vigour was estimated by employing a handheld GreenSeeker® NDVI sensor (Trimble Inc., Westminster, Colorado, USA) during BBCH 71–81 (Lorenz *et al.*, 1995). The instrument was positioned 1 m below and parallel to the angled overhead Pergola canopy, while a white reflective board was placed above the canopy to reflect any sensor signals passing through canopy gaps, as described in Drissi *et al.* (2009) (Figure S2). Sensing was conducted at moderate to nearly fully developed leaf area between BBCH 71 and 81 (Lorenz *et al.*, 1995), with 10 replicates per block.

4. Remote sensors

4.1. Airborne imagery

The studied vineyards were investigated by a DJI Matrice 600 Pro unmanned aerial vehicle (UAV) (Z DJI Technology Co., Ltd, Shenzhen, Guangdong, China) equipped with MicaSense RedEdge-MX multispectral camera (MicaSense, Inc., Seattle, Washington, USA). The flights were conducted on 02 July 2022 for Nassar vineyard and on 24 June 2023 and 08 June 2024 for Pedemonte vineyard in the daytime (10:00–15:00). The aerial survey was conducted parallel to the ground at a flight speed of 3 m/s, an altitude of 40 m above ground level, and a ground sampling distance of 3 cm/pixel, and using forward and side overlap settings of 70 %. Imaging was performed using a camera equipped with an array of sensors and band-pass filters centered at 475 nm (Blue), 560 nm (Green), 668 nm (Red), 717 nm (Red Edge), and 842 nm (NIR). PIX4Dfields software (Pix4D SA) was used for radiometric calibration and orthomosaics generation. The orthomosaics were then aligned in the QGIS software environment (Version 3.16.16, Hannover, Germany) using four ground control point coordinates acquired by a Trimble® R2 global navigation satellite system (Trimble Inc., Westminster, Colorado, USA). The digital elevation model (DEM) was obtained for each vineyard. To discriminate between canopy pixels and non-canopy ones, SAGA *k*-means Clustering for Raster tool (Conrad *et al.*, 2015), guided by MSAVI and MCARI indices, was applied on the NDVI raster (Table S1). The clusters containing no-canopy pixels were filtered out, leaving only canopy pixels. A 0.5 m point grid was established over the filtered NDVI raster, and the NDVI values were extracted for each point and interpolated within the vineyard boundaries using ordinary kriging to generate a continuous map based solely on canopy pixels. This map was classified into three categories (high,

medium, and low vigour) using a Quantile classification method. NDVI values were averaged per block, considering only canopy pixels, and the number of canopy pixels per block was calculated to estimate the canopy dimension as observed from above (2D canopy).

4.2. Satellite imagery

Sentinel-2 level-2 A (MSIL2A) satellite imagery was downloaded from the Copernicus Open Access Hub (European Space Agency). One set of images was selected to match the dates closest to the UAV flights, from which the NDVI was calculated. A second set of images was used to calculate the NDWI (Table S1). Image acquisition dates coincided with the VWC measurements, except in three cases in which images were acquired within three days of the VWC measurements. These dates were carefully selected to ensure they were periods without precipitation or significant temperature changes. All acquisition dates are summarised in Supplementary dataset S1. The indices were resampled as needed to obtain 10 m/pixel resolution and aligned using the Georeferencer tool in the QGIS software environment (Version 3.16.16, Hannover, Germany), using the same GCPs as previously described.

5. Statistical analyses

Analyses were done employing R Studio environment (R Core Team, 2021). Measurements taken within each block were averaged to obtain one representative value, and each block was treated as an independent experimental unit. Parameters collected for each vineyard were analysed separately for each year. Data was analysed by pair-wise Pearson's correlation and presented as a correlation matrix using the *corrplot* package (Simko, 2021). Given the limited sample sizes (n = 6 for Pedemonte and n = 8 for Nassar), formal assessment of distributional assumptions was not informative; hence, correlation analyses were interpreted cautiously. To account for multiple testing, *p*-values were adjusted using the Benjamini–Hochberg false discovery rate (FDR) procedure. Hierarchical clustering analysis (HCA) was conducted using Pearson's correlations as the distance measure and visualised as dendrograms using the base R package. The coefficient of variation (CV) was calculated for each parameter. A linear mixed-effects model (LMM) was fitted to evaluate the sensitivity of NDWI to VWC variations using the lme4 package, with significance assessed using the *lmerTest* package. Block-level data collected from vines and berries were interpolated across the vineyards using the inverse distance weighting (IDW) method, which is suitable for a small sample size, and classified using the Quantile classification method within the QGIS software environment (Version 3.16.16, Hannover, Germany).

RESULTS

1. Weather conditions

Weather data was recorded during the period 2022–2024 from 01 April to 31 October by a weather station located at Castelrotto (Verona, north-east Italy; 45°29'58.91" N, 10°53'56.03" E) (Figures S1A, B and C), which is situated approximately 4 km from both study vineyards. Year 2023 was characterised by excessive heat, reaching the highest cumulative GDD of 2040 °C, compared to 1947 °C in 2022 and 1970 °C in 2024 (Figure S1D). Despite being the warmest year, 2023 experienced multiple rainfall events with a total of 768 mm, which were relatively well distributed throughout the season. Comparable rainfalls were registered in 2024 (760 mm), whereas 2022 was particularly drier, receiving only 341 mm of rainfall.

2. Pedemonte vineyard

The Pedemonte vineyard, characterised by an elongated and narrow layout, was monitored during the 2023 and 2024 growing seasons. The data collected are summarised at the block level in Supplementary dataset S1. The DEM shows a gently undulating terrain (Figure 1A), the elevation gradually decreasing from northeast to southwest (1.5 %) and slightly increasing just south of the dirt road dividing the vineyard. In 2023, the UAV NDVI map showed a general decrease in vigour along the terrain's main slope (Figure 1B), with a CV of 2.5 % between blocks (Supplementary dataset S1), while in 2024, there was a shift in the lowest NDVI values towards the dirt road (Figure 1C) and the CV was reduced to 1 %. Quantile classification on UAV NDVI data indicated comparable NDVI intervals for the low-vigour class in both years (0.857–0.865 in 2023; 0.859–0.865 in 2024), whereas the medium- and high-vigour classes exhibited markedly narrower ranges in 2024. Specifically, the medium-vigour class shifted from 0.866–0.873 in 2023 to 0.863–0.864 in 2024, and the high-vigour class from 0.874–0.880 in 2023 to 0.865–0.866 in 2024 (Figures 1D and E). Sentinel-2 NDVI data generally presented higher between-block CVs compared to UAV NDVI, and confirmed the lower vigour variability in 2024, with a lower CV (2.5 %) compared to 2023 (6.6 %) (Supplementary dataset S1). Sentinel-2 NDVI maps generally followed the trends of the UAV NDVI maps, successfully detecting interannual modifications in vigour patterns (Figures 1F and G).

2.1. Relationship between sensor data and vine and berry measurements

Consistent with the decrease observed from 2023 to 2024 in remotely sensed NDVI, several parameters associated with vigour also showed reduced variability in 2024, including ground-based NDVI, yield, and berry weight (Supplementary dataset S1). Other berry parameters also decreased in CV values, such as TSS, anthocyanins, polyphenols, and CWSI. By contrast, 2D canopy, bud fruitfulness, skin thickness, acidity, pH, and VWC did not show the same reduction in variability, and some even showed a marked increase in CV. In both years, HCA divided the parameters into two main branches (Figures 2A and B): one grouped all three NDVIs, 2D canopy, bud fruitfulness, yield, berry weight, VWC, and TA, and showed relatively high and stable internal cohesion ($d \approx 0.5$; 2023, $d \approx 0.4$; 2024); the other grouped anthocyanins, polyphenols, CWSI and pH parameters, showing comparable associations in 2023 ($d \approx 0.5$) and weaker cohesion in 2024 ($d \approx 0.8$). Within each branch, tighter relationships among specific parameters were consistently observed across

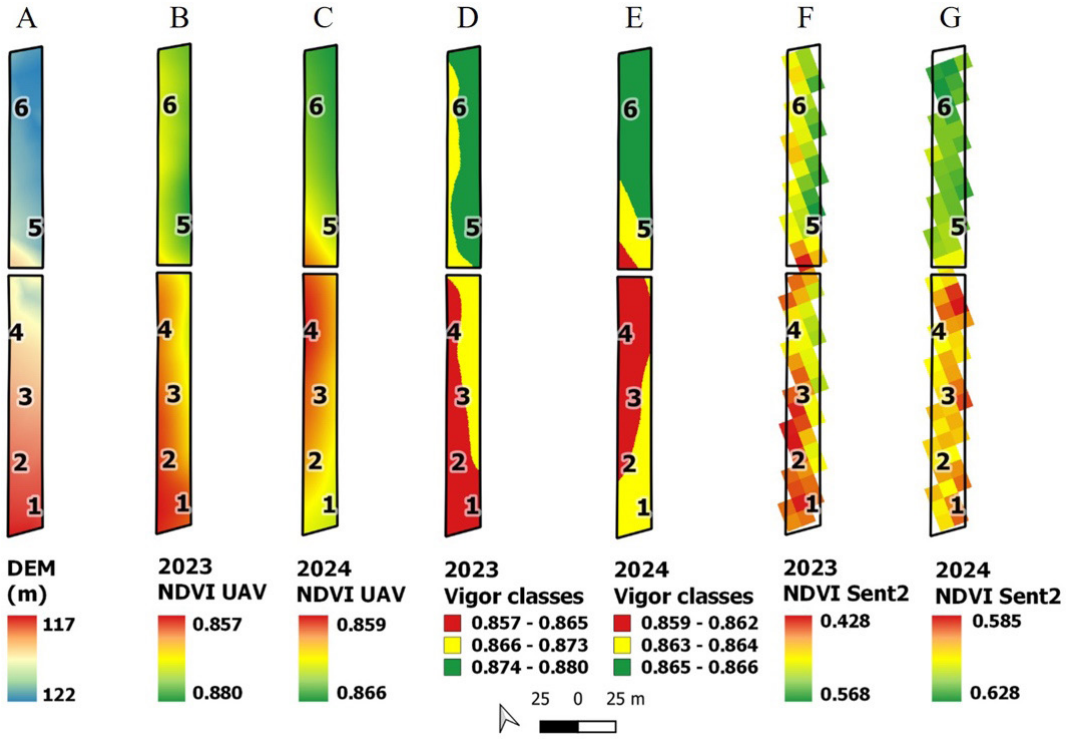


FIGURE 1. Remote sensing in Pedemonte vineyard during 2023–2024.

A. Digital elevation model (DEM). B-C. NDVI maps obtained from UAV imagery (NDVI UAV). D-E. Vigour class maps derived from UAV NDVI data. F-G. NDVI maps obtained from Sentinel-2 imagery (NDVI Sent2). Numbers indicate the six blocks monitored.

years, such as between VWC and berry weight ($d \approx 0.1$), with significant positive correlation in 2024 ($r = 0.95$; $q \leq 0.05$, Figure 2D), and between CWSI and pH ($d < 0.1$) (Figures 2A and B), with significant positive correlations in 2023 ($r = 0.95$; $q \leq 0.05$, Figure 2C). Parameters located on opposite main dendrogram branches generally exhibited negative inter-cluster correlations. In particular, pH and CWSI showed stronger and more consistent negative relationships with most parameters in the opposing branch, whereas berry parameters such as TSS, anthocyanins, and polyphenols displayed weaker and less consistent negative associations with those same parameters.

Interpolated maps based on block-level data were used to facilitate visual comparison of variability among blocks, across parameters, and between seasons. Although derived from a limited number of blocks, most of the maps aligned with patterns derived from remote sensing data and consistently indicated a north-south variability gradient in both years (Figure 3).

2.2. Assessment of Sentinel-2 sensitivity to soil moisture

The sensitivity of Sentinel-2 to physical vineyard variations was evaluated using repeated NDWI measurements across the two years and ground-truthed against VWC data (Supplementary dataset S1). Soil moisture and canopy water status were selected, because changes in soil moisture directly influence canopy water status and their values vary non-directionally throughout the season, unlike vigour measurements, which tend to increase over time and whose signals may become saturated (Curran *et al.*, 1983). NDWI was plotted against VWC in a single plot including all sampling dates; the corresponding trend lines were largely parallel, indicating date-dependent variability in the relationship (Figure S3). To account for this variability, as well as for repeated sampling within the same six blocks, an LME model was used to evaluate the relationship between NDWI and VWC, including these sources of variability as random effects in the following model:

$$\text{NDWI} \sim \text{VWC} + (1 \mid \text{Block}) + (1 \mid \text{Date})$$

The LME results showed that NDWI responded significantly to changes in VWC, but the effect was weak, indicating low sensitivity ($\beta = 0.00227 \pm 0.00052$ SE, $p < 0.001$) (Table S2). Variance partitioning showed that sampling date explained most NDWI variability (0.00749), while block effects were minimal (0.00011). VWC and NDWI interpolated maps visually represented block-level data distribution in the vineyard and showed strong pattern similarities between the two parameters, both within and between seasons (Figure 4). Notably, the VWC and NDWI-derived maps showed high pattern similarities with CWSI-interpolated data in both monitored years (Figure 3).

3. Nassar vineyard

The Nassar multivarietal vineyard included four cultivar plots (cv. Corvina, Corvinone, Rondinella, and Molinara) (Figure 5A) monitored during the 2022 growing season. The data collected are summarised at the block level in Supplementary dataset

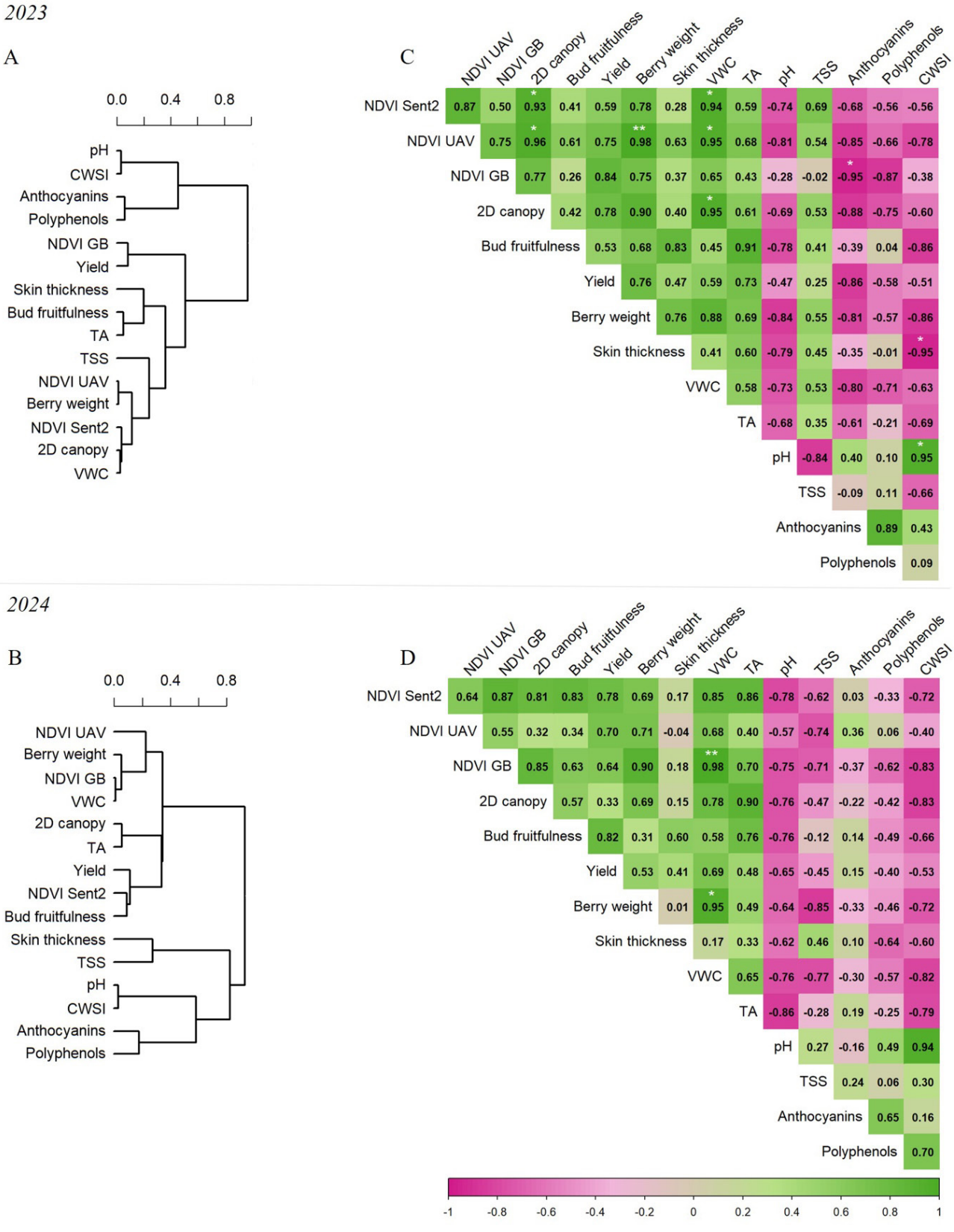


FIGURE 2. Correlation analyses between parameters measured in Pedemonte vineyard during 2023–2024.

A-B. Hierarchical clustering analysis using Pearson's coefficients as a distance. C-D. Pearson's correlation coefficient (r) matrices. Asterisks represent statistically significant correlations after Benjamini–Hochberg False Discovery Rate (FDR) correction ($q \leq 0.05$ = *; $q \leq 0.01$ = **) based on t-test. Sent2 = Sentinel-2. GB = Ground-based.

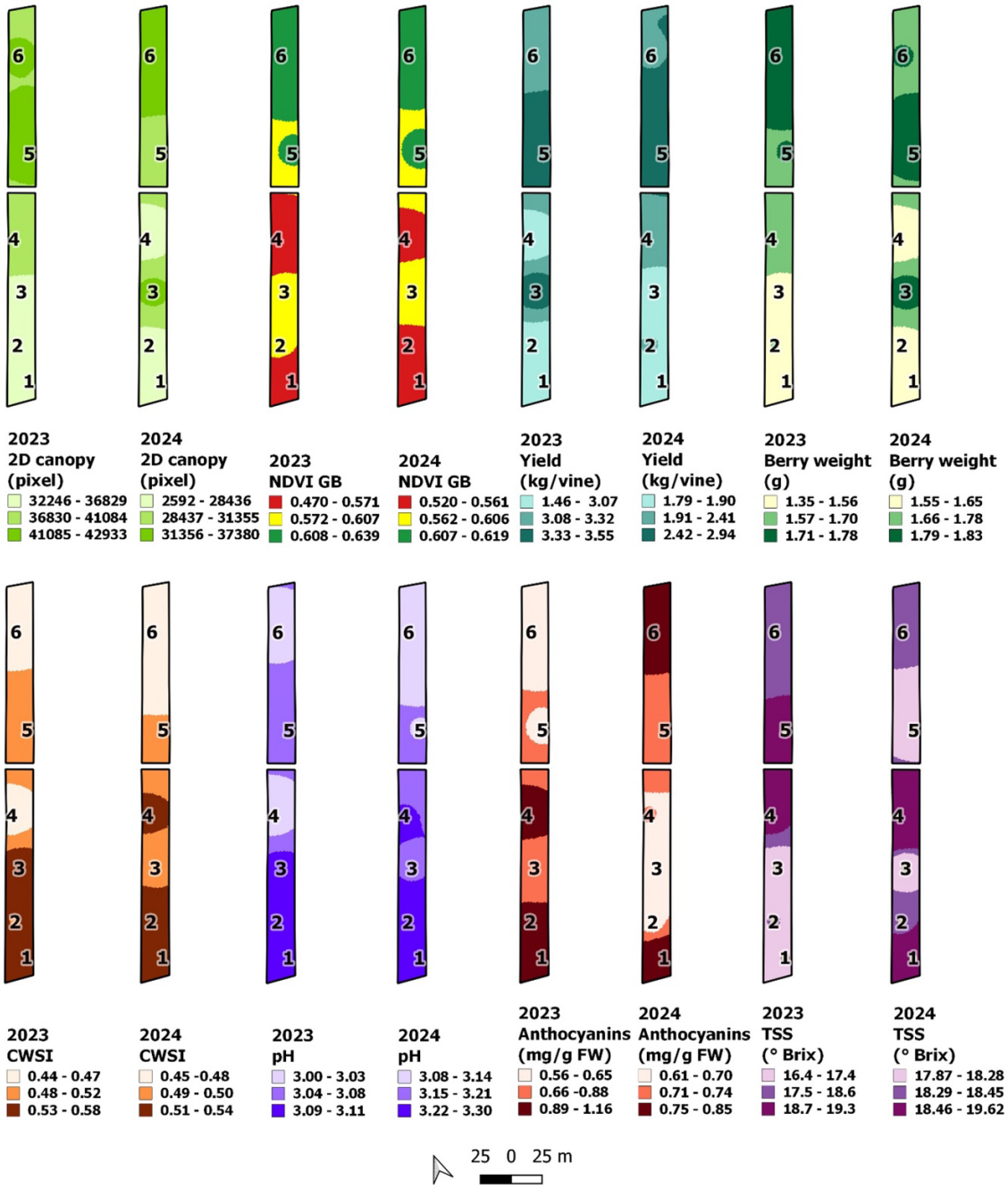


FIGURE 3. Interpolated maps of Pedemonte vineyard during 2023–2024.

Each map displays interpolated values of the measured parameters derived from six vineyard blocks, indicated with numbers. GB = Ground-based.

S1. The DEM indicated a slight topographic slope of about 1.25 % from the north-west to the south-east (Figure 5B). By contrast, the UAV NDVI map revealed a vigour gradient increasing from the north-east to the south-west, orthogonal to the slope, with between-block CVs of about 2 % (Figure 5C). The classification of the vineyard into three vigour classes highlighted a spatial pattern that was independent of the cultivar plot layout (Figure 5D). The Sentinel-2 NDVI map showed a similar trend to the UAV NDVI map, although it exhibited higher between-block variability (CV ≈ 14 %) (Figure 5E).

3.1. Relationship between sensor data and vine and berry measurements

HCA identified a tight clustering ($d \approx 0.2$) between vigour-related data obtained from sensors (*e.g.*, three NDVIs, 2D canopy), direct canopy measurements (leaf area, shoot elongation rate, pruning weight), and yield (Figure 5F). The strongest association was found between 2D canopy and Sentinel-2 NDVI ($r = 1.00$; $q < 0.001$); pruning weight was also strongly correlated with Sentinel-2 NDVI ($r = 0.90$; $q < 0.05$), yield ($r = 0.89$; $q < 0.05$) and 2D canopy ($r = 0.88$;

$q < 0.05$). In addition, UAV- and ground-based NDVI showed strong associations with shoot elongation rate ($r = 0.97$; $q < 0.01$ and $r = 0.93$; $q < 0.05$, respectively) (Figure 5G). TA, often associated with high vigour and strongly influenced by varietal effects, resulted as an outlier within the vigour branch ($d \approx 0.5$) (Figure 5F). A separate tight cluster ($d \approx 0.2$) grouped traits more strongly influenced by varietal characteristics, including anthocyanins, polyphenols, skin thickness, and berry weight, along with VWC, the only non-cultivar-related parameter in this cluster. Two additional compact clusters ($d \approx 0.2$), TSS with bud fruitfulness and pH with CWSI were positioned apart from the main groups, indicating that these traits operate independently from the main vigour- and varietal-related clusters.

Block-level interpolated maps further highlighted that vine-level parameters (*e.g.*, ground-based NDVI, shoot kinetics, pruning weight, yield, bud fruitfulness, and CWSI) together with VWC, exhibited spatial patterns consistent with those detected by the remote sensors (Figure 5H). By contrast, spatial maps of berry traits (*e.g.*, berry weight, skin thickness, anthocyanin content, TA, and pH) did not align with those of the vigour-related parameters and partially followed the cultivar plot (Figure 5H). Berry weight, skin thickness, and anthocyanin content were higher in the Corvinone plot, consistent with its large fruit morphology and phenolic profile. Conversely, TSS showed higher concentration in the Corvina plot, consistent with early ripening of this cultivar compared to the other three. The TA map partially reflected varietal

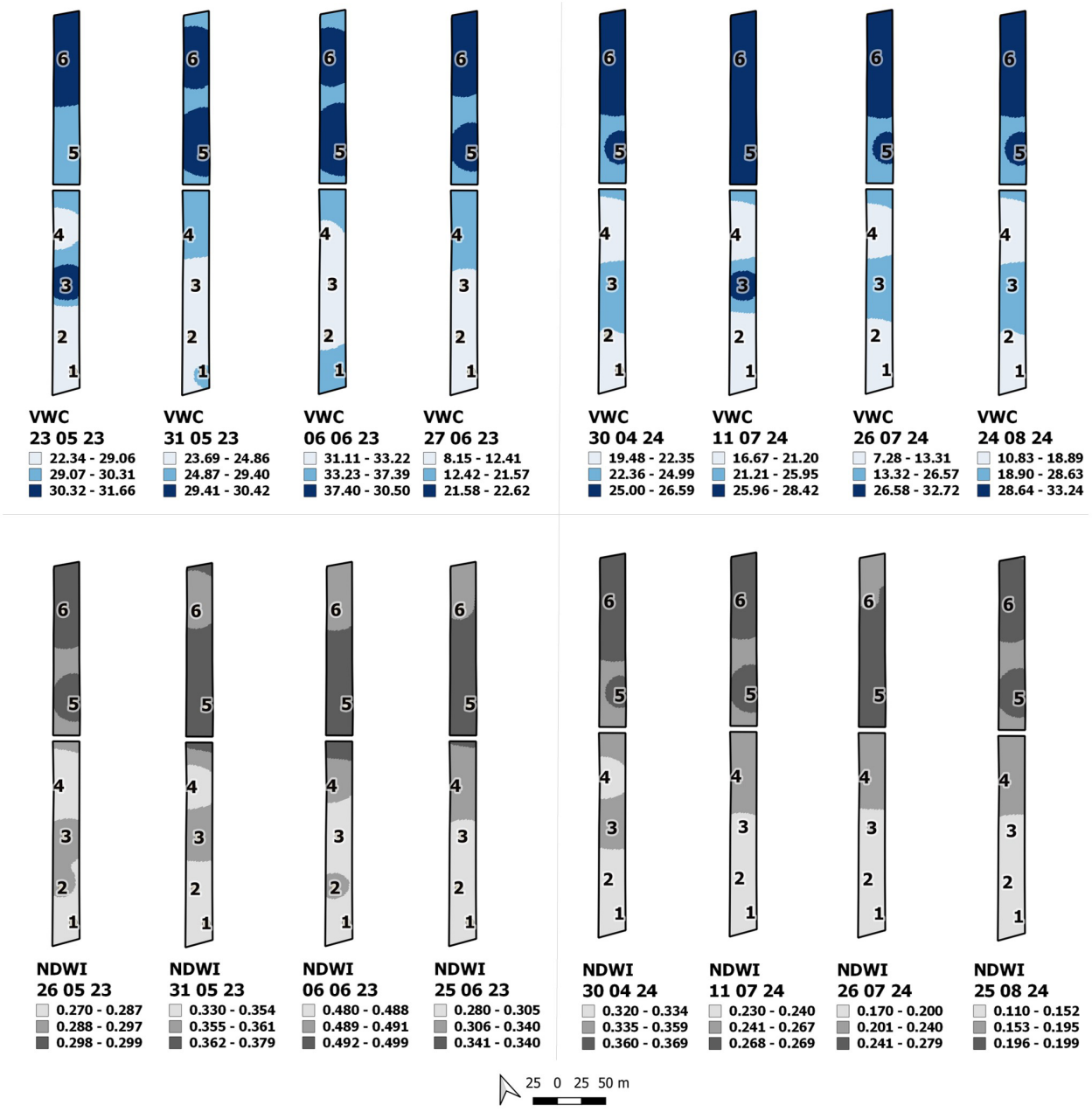


FIGURE 4. Water distribution in Pedemonte vineyard over two consecutive seasons.

Block-level interpolated maps of VWC derived from ground-based TDR soil moisture sensor measurements (upper panel) and NDWI derived from Sentinel-2 imagery (lower panel).

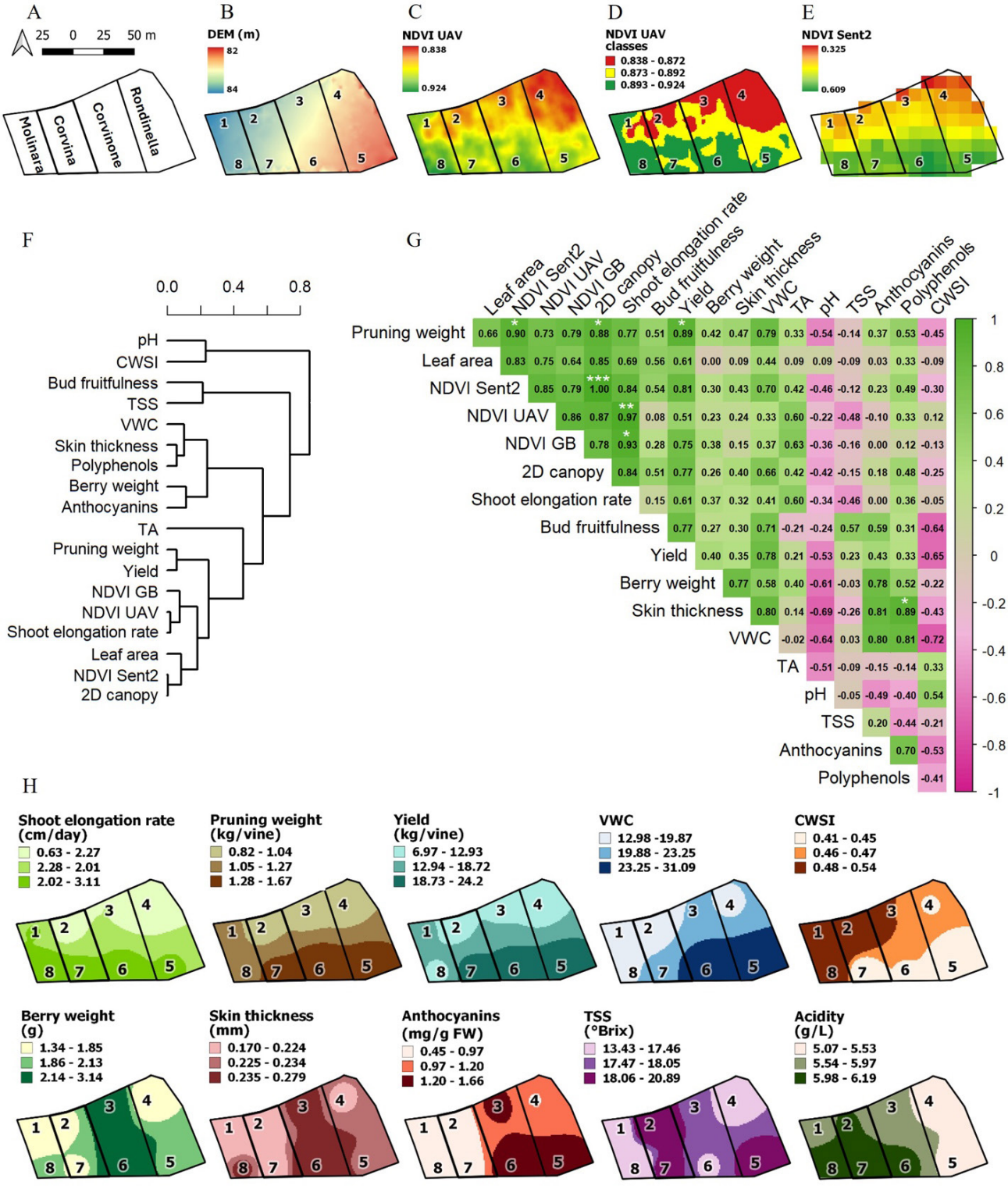


FIGURE 5. Spatial variability of Nassar vineyard.

A. Map of cultivar plots. B. Digital elevation model (DEM). C. NDVI maps obtained from UAV imagery (NDVI UAV). D. Vigour class maps derived from UAV NDVI data. E. NDVI maps obtained from Sentinel-2 imagery (NDVI Sent2). Numbers indicate eight blocks monitored across four cultivar plots. F. Hierarchical clustering analysis using Pearson's coefficients as a distance. G. Pearson's correlation coefficient (r) matrix. Asterisks represent statistically significant correlations after Benjamini–Hochberg false discovery rate (FDR) correction ($q \leq 0.05$ = *; $q \leq 0.01$ = **; $q \leq 0.001$ = ***), based on t-test. H. Interpolated maps of parameter values measured in eight vineyard blocks. Sent2 = Sentinel-2. GB = Ground-based.

influence, showing the lowest TA values in Rondinella berries, but also mirrored the vigour variation across the vineyard, with higher TA values observed in the south-eastern area.

DISCUSSION

This study evaluated the efficiency of established precision viticulture methods in detecting intra-parcel variability within vineyards of the Valpolicella wine region, an area that has received limited attention using such approaches.

The discontinuous vine canopy complicates the application of top-down, sensor-based methods, as it requires the canopy to be distinguished from the background. This challenge is further aggravated by the small parcel size, irregular geometry, and inter-row cover crops that characterise Valpolicella vineyards. Having a large pixel size, low-resolution sensors inevitably capture both canopy and non-canopy elements, introducing noise and reducing measurement precision (De Petris *et al.*, 2024; Khaliq *et al.*, 2019; Zsigmond *et al.*, 2025). High-resolution sensors may enable more effective isolation of canopy pixels, which can then be interpolated to reconstruct continuous, canopy-based spatial representations (Sozzi *et al.*, 2020). However, in cover-cropped vineyards, separating the canopy from the background remains challenging even at high resolution. Moreover, in small vineyards with irregular shapes, high-resolution data may still result in the limited and uneven sampling of canopy pixels, thereby reducing the robustness of spatial interpolation.

Despite these structural and methodological limitations, the Sentinel-2 NDVI map, with its relatively coarse spatial resolution (10 m pixel^{-1}), showed spatial patterns similar to those derived from UAV NDVI maps interpolated from canopy pixels (3 cm pixel^{-1}), even though the between-block variability was higher in Sentinel-2 NDVI data, probably due to mixed pixels capturing non-canopy elements. These parameters also exhibited several statistically significant correlations with each other and with the 2D canopy parameter (*i.e.*, the number of canopy pixels), indicating their consistency in detecting vigour variability in the monitored vineyards. A stable relationship between Sentinel-2-derived canopy water status and soil moisture across two seasons in Pedemonte vineyard further supports the ability of low-resolution imagery to capture spatial patterns. However, this relationship lacked sufficient sensitivity for the accurate estimation of absolute soil water content for irrigation management. A possible explanation for the high correspondence between the remote sensor parameters lies in the canopy architecture of the Pergola trellis system, which is oriented nearly parallel to the sensor plane. This configuration increases the canopy visibility to a top-down sensor while reducing interference from inter-row cover crops. As a result, the signal from the canopy is enhanced, reducing noise and improving sensor performance even at lower resolutions. A direct comparison with vertically trained systems, such as vertical shoot positioning, would help validate this hypothesis.

By contrast, while the Pergola system may favour top-down remote sensing, it limits the applicability of ground-based canopy sensors. The elevated overhead canopy restricts access to the sun-exposed curtain, which is required for certain measurements, such as canopy temperature acquisition using thermal cameras (Grant *et al.*, 2016). It also complicates the use of active handheld NDVI sensors, which require a white reference panel behind the canopy (Drissi *et al.*, 2009). This structure also constrains machinery access by limiting the feasibility of on-the-go ground-based sensing and reducing both data volume and precision (Bono *et al.*, 2026; Tardaguila *et al.*, 2021). In our study, ground-based sensing methods were adapted to these constraints; however, while they provided consistent results relative to ground-truth measurements, they were time-consuming, potentially operator-dependent, and less suitable for large-scale applications. As a result, this could reduce statistical accuracy.

A key strength of this study lies in the integration of a multi-sensor approach, combining information on vine vigour and water status with complementary vine- and berry-based measurements. This resulted in a comprehensive dataset that enabled vineyard variability to be examined from multiple perspectives.

The Pedemonte vineyard was monitored across two seasons, and despite limited NDVI ranges, several relevant agronomical and oenological parameters correlated with NDVI (*e.g.*, yield, VWC, TSS, and anthocyanins) showed substantial variation between blocks, while other parameters exhibited stable relationships. Bud fruitfulness reflects early-season reproductive potential (Reynolds, 2010) and was linked to the final product parameters. Yield and berry weight, aligned with early-season vigour indices, showed strong relationships with TA and pH, but weaker associations with TSS, polyphenols, and anthocyanins, indicating that vigour variability only partially translated into berry composition. The tendency of vigorous vines to maintain higher berry TA has been previously reported (Dorin *et al.*, 2024; Ferro *et al.*, 2023), and a stronger association between TA and vine vigour compared to TSS has been reported (Di Gennaro *et al.*, 2019; Ferrer *et al.*, 2020). Besides being highly responsive to vigour variation, pH had strong associations with CWSI. Water stress may increase K^+ accumulation in berries through upregulation of transport mechanisms, contributing to higher pH. In fact, the upregulation of the K^+ channel *VvK1.1* gene was observed in berry phloem vasculature under drought conditions (Cuéllar *et al.*, 2010). Although direct physiological measurements of water status were not included, the agreement between these sensor-derived parameters supports their reliability in assessing vine water status, in line with previous findings (Ru *et al.*, 2020).

VWC and CWSI also proved informative for berry morphology. VWC was positively associated with berry weight, while CWSI was negatively associated with both skin thickness and berry weight. Berry morphology is particularly critical in Valpolicella berries intended for post-harvest dehydration before vinification, where skin thickness strongly influences dehydration kinetics and

final wine quality (Rolle *et al.*, 2012). During ripening, berry softening and expansion may lead to skin thinning (Hardie *et al.*, 1996), whereas under water deficit conditions, skin thickening has been reported (Porro *et al.*, 2010). These contrasting mechanisms may explain the weak relationships observed between berry skin thickness and vine vigour parameters. Low-vigour vines may develop thinner berry skins due to accelerated ripening dynamics; however, when low vigour is driven by water deficit, stress-induced skin thickening may occur instead. The consistent inverse relationship between skin thickness and CWSI observed in this study suggests that, in the Pedemonte vineyard, berries from areas with higher CWSI were more influenced by accelerated ripening dynamics than by stress-induced thickening. Additionally, the Pergola trellis architecture may play a role. The horizontal canopy curtain is highly exposed to solar radiation, while clusters remain shaded beneath it. This configuration may decouple canopy temperature from cluster thermal conditions, implying that high canopy CWSI does not necessarily correspond to berry-level stress.

Another defining characteristic of Valpolicella is the combined vinification of the autochthonous cultivars to produce local wines. Given their shared use, these cultivars are often grown side by side and managed as a single unit. This raises the question of whether precision viticulture methods should be applied collectively across cultivar plots or tailored to individual cultivars. In the multivarietal Nassar vineyard, vigour indices and vine agronomic parameters exhibited spatial patterns that were not associated with cultivar distribution, whereas several berry-related traits showed clear cultivar-dependent patterns. This indicates that berry trait variability was primarily driven by cultivar rather than site-specific agronomic conditions. Accordingly, while NDVI-based approaches remain effective for agronomic characterisation in multivarietal Valpolicella vineyards, their ability to capture cultivar-specific berry traits is limited unless variety-specific models are developed.

CONCLUSIONS

This study provides a preliminary assessment of the feasibility and challenges associated with applying sensor-based approaches in the distinctive viticultural area of Valpolicella.

Analyses of the extensive dataset revealed relationships between sensor-derived parameters and vine and berry traits. These included expected correlations (*e.g.*, NDVI and berry acidity, VWC, and berry weight), as well as associations between traits of particular relevance for the Valpolicella area (*e.g.*, CWSI and skin thickness). Notably, the use of a relatively low-resolution sensor such as Sentinel-2 proved effective even in the small vineyards typical of the region. This performance may be attributed to the Pergola trellis system, whose horizontally-developed canopy reduces background interference for top-down sensing.

Beyond confirming known pairwise relationships at the regional scale, this study highlights the value of an integrated, multi-sensor approach combining complementary indicators of vine vigour and water status. Such an approach enhances the applicability of precision viticulture methodologies in viticultural regions with similar structural and management characteristics.

ACKNOWLEDGEMENTS

Bolla S.p.A., Speri Viticoltori S.S., Marco Orso, Andrea Piccino, SMACT Competence Center.

REFERENCES

Accordini, D. (2013). Amarone. In *Sweet, Reinforced and Fortified Wines* (pp. 187-203). https://doi.org/10.1002/9781118569184.ch13

Ammoniaci, M., Kartsiotis, S.-P., Perria, R., & Storchi, P. (2021). State of the Art of Monitoring Technologies and Data Processing for Precision Viticulture. *Agriculture*, *11*(3), 201. https://doi.org/10.3390/agriculture11030201

Bonilla, I., Martínez de Toda, F., & Martínez-Casasnovas, J. A. (2015). Unexpected relationships between vine vigor and grape composition in warm climate conditions. *OENO One*, *49*(2), 127-136. https://doi.org/10.20870/oeno-one.2015.49.2.87

Bono, A., Guaragnella, C., & D'Orazio, T. (2026). A perspective analysis of imaging-based monitoring systems in precision viticulture: Technologies, intelligent data analyses and research challenges. *Artificial Intelligence in Agriculture*, *16*(1), 62-84. https://doi.org/10.1016/j.aiia.2025.08.001

Bramley, R. G. V., Ouzman, J., Trought, M. C. T., Neal, S. M., & Bennett, J. S. (2019). Spatio-temporal variability in vine vigour and yield in a Marlborough Sauvignon Blanc vineyard. *Australian Journal of Grape and Wine Research*, *25*(4), 430-438. https://doi.org/10.1111/ajgw.12408

Conrad, O., Bechtel, B., Bock, M., Dietrich, H., Fischer, E., Gerlitz, L., Wehberg, J., Wichmann, V., & Böhner, J. (2015). System for Automated Geoscientific Analyses (SAGA) v. 2.1.4. *Geoscientific Model Development*, *8*(7), 1991-2007. https://doi.org/10.5194/gmd-8-1991-2015

Cuéllar, T., Pascaud, F., Verdeil, J.-L., Torregrosa, L., Adam-Blondon, A.-F., Thibaud, J.-B., Sentenac, H., & Gaillard, I. (2010). A grapevine Shaker inward K+ channel activated by the calcineurin B-like calcium sensor 1–protein kinase CIPK23 network is expressed in grape berries under drought stress conditions. *The Plant Journal*, *61*(1), 58-69. https://doi.org/10.1111/j.1365-313X.2009.04029.x

Curran, P. J., Steven, M. D., Houghton, J. T., Cook, A. H., & Charnock, H. (1983). Multispectral remote sensing for the estimation of green leaf area index. *Philosophical Transactions of the Royal Society of London. Series A, Mathematical and Physical Sciences*, *309*(1508), 257-270. https://doi.org/doi:10.1098/rsta.1983.0039

De Petris, S., Sarvia, F., Parizia, F., Ghilardi, F., Farbo, A., & Borgogno-Mondino, E. (2024). Assessing mixed-pixels effects in vineyard mapping from Satellite: A proposal for an operational solution. *Computers and Electronics in Agriculture*, *222*, 109092. https://doi.org/10.1016/j.compag.2024.109092

Di Gennaro, S. F., Dainelli, R., Palliotti, A., Toscano, P., & Matese, A. (2019). Sentinel-2 Validation for Spatial Variability Assessment in Overhead Trellis System Viticulture Versus UAV and Agronomic Data. *Remote Sensing*, *11*(21), 2573. https://doi.org/10.3390/rs11212573

Di Stefano, R., & Cravero, M. (1991). Metodi per lo studio dei polifenoli dell'uva. *Rivista di Viticoltura e di Enologia*, *44*.

Dorin, B., Reynolds, A. G., Lee, H.-S., Carrey, M., Shemrock, A., & Shabanian, M. (2024). Detecting cool-climate Riesling vineyard variation using unmanned aerial vehicles and proximal sensors. *Drone Systems and Applications*, *12*, 1-18. https://doi.org/10.1139/dsa-2023-0024

Drissi, R., Goutouly, J.-P., Forget, D., & Gaudillere, J.-P. (2009). Nondestructive Measurement of Grapevine Leaf Area by Ground Normalized Difference Vegetation Index. *Agronomy Journal*, *101*(1), 226-231. https://doi.org/10.2134/agronj2007.0167

Ferrer, M., Echeverría, G., Pereyra, G., Gonzalez-Neves, G., Pan, D., & Mirás-Avalos, J. M. (2020). Mapping vineyard vigor using airborne remote sensing: relations with yield, berry composition and sanitary status under humid climate conditions. *Precision Agriculture*, *21*(1), 178-197. https://doi.org/10.1007/s11119-019-09663-9

Ferro, M. V., & Catania, P. (2023). Technologies and Innovative Methods for Precision Viticulture: A Comprehensive Review. *Horticulturae*, *9*(3), 399. https://doi.org/10.3390/horticulturae9030399

Ferro, M. V., Catania, P., Miccichè, D., Pisciotta, A., Vallone, M., & Orlando, S. (2023). Assessment of vineyard vigour and yield spatio-temporal variability based on UAV high resolution multispectral images. *Biosystems Engineering*, *231*, 36-56. https://doi.org/10.1016/j.biosystemseng.2023.06.001

Grant, O., Ochagavía, H., Baluja, J., Diago, M.-P., & Tardaguila, J. (2016). Thermal imaging to detect spatial and temporal variation in the water status of grapevine (Vitis Vinifera L.). *Journal of Horticultural Science and Biotechnology*, *91*, 44-55. https://doi.org/10.1080/14620316.2015.1110991

Hardie, W. J., O'Brien, T. P., & Jaudzems, V. G. (1996). Morphology, anatomy and development of the pericarp after anthesis in grape, Vitis vinifera L. *Australian Journal of Grape and Wine Research*, *2*(2), 97-142. https://doi.org/10.1111/j.1755-0238.1996.tb00101.x

Harvey, P. (2016). *ExifTool*. In https://exiftool.org/

Jones, H. G., Stoll, M., Santos, T., Sousa, C. D., Chaves, M. M., & Grant, O. M. (2002). Use of infrared thermography for monitoring stomatal closure in the field: Application to grapevine [Article]. *Journal of Experimental Botany*, *53*(378), 2249-2260. https://doi.org/10.1093/jxb/erf083

Khaliq, A., Comba, L., Biglia, A., Ricauda Aimonino, D., Chiaberge, M., & Gay, P. (2019). Comparison of Satellite and UAV-Based Multispectral Imagery for Vineyard Variability Assessment. *Remote Sensing*, *11*(4), 436. https://doi.org/10.3390/rs11040436

Ledderhof, D., Reynolds, A. G., Brown, R., Jollineau, M., & Kotsaki, E. (2017). Spatial Variability in Ontario Pinot noir Vineyards: Use of Geomatics and Implications for Precision Viticulture. *American Journal of Enology and Viticulture*, *68*(2), 151-168. https://doi.org/10.5344/ajev.2016.16062

Loggenberg, K., Strever, A., & Münch, Z. (2024). Scoping the Field: Recent Advances in Optical Remote Sensing for Precision Viticulture. *ISPRS International Journal of Geo-Information*, *13*(11), 385. https://doi.org/10.3390/ijgi13110385

Lorenz, D. H., Eichhorn, K. W., Bleiholder, H., Klose, R., Meier, U., & Weber, E. (1995). Growth Stages of the Grapevine: Phenological growth stages of the grapevine (Vitis vinifera L. ssp. vinifera)—Codes and descriptions according to the extended BBCH scale. *Australian Journal of Grape and Wine Research*, *1*(2), 100-103. https://doi.org/10.1111/j.1755-0238.1995.tb00085.x

Mizik, T. (2023). How can proximal sensors help decision-making in grape production? *Heliyon*, *9*(5). https://doi.org/10.1016/j.heliyon.2023.e16322

Porro, D., Ramponi, M., Tomasi, T., Rolle, L., & Poni, S. (2010). Nutritional implications of water stress in grapevine and modifications of mechanical properties of berries. *Acta horticulturae 868*, 73-80. https://doi.org/10.17660/ActaHortic.2010.868.5

R Core Team. (2021). *A Language and Environment for Statistical Computing*. In R Foundation for Statistical Computing. http://www.R-project.org

Reynolds, A. (2010). Viticultural and vineyard management practices and their effects on grape and wine quality. In A. G. Reynolds (Ed.), Managing wine quality: Viticulture and wine quality (pp. 365-444). https://doi.org/10.1533/9781845699284.3.365

Rolle, L., Siret, R., Segade, S., Maury, C., Gerbi, V., & Jourjon, F. (2012). Instrumental Texture Analysis Parameters as Markers of Table-Grape and Winegrape Quality: A Review. *American Journal of Enology and Viticulture*, *63*, 11-28. https://doi.org/10.5344/ajev.2011.11059

Ru, C., Hu, X., Wang, W., Ran, H., Song, T., & Guo, Y. (2020). Evaluation of the Crop Water Stress Index as an Indicator for the Diagnosis of Grapevine Water Deficiency in Greenhouses. *Horticulturae*, *6*(4), 86. https://doi.org/10.3390/horticulturae6040086

Simko, T. W. a. V. (2021). *R package 'corrplot': Visualization of a Correlation Matrix*. https://github.com/taiyun/corrplot

Sozzi, M., Kayad, A., Marinello, F., Taylor, J., & Tisseyre, B. (2020). Comparing vineyard imagery acquired from Sentinel-2 and Unmanned Aerial Vehicle (UAV) platform. *OENO One*, *54*(2), 189-197. https://doi.org/10.20870/oeno-one.2020.54.1.2557

Squeri, C., Diti, I., Rodschinka, I., Poni, S., Dosso, P., Scotti, C., & Gatti, M. (2021). Is Precision Viticulture Beneficial for the High-Yielding Lambrusco (Vitis Vinifera L.) Grapevine District? *American Journal of Enology and Viticulture*, *72*, 267-278. https://doi.org/10.5344/ajev.2021.20060

Tardaguila, J., Stoll, M., Gutiérrez, S., Proffitt, T., & Diago, M. P. (2021). Smart applications and digital technologies in viticulture: A review. *Smart Agricultural Technology*, *1*, 100005. https://doi.org/10.1016/j.atech.2021.100005

Tattersall, G. J. (2021). *Thermimage: Thermal Image Analysis*. In https://cran.r-project.org/package=Thermimage

Zanchin, A., Cogato, A., Sozzi, M., Tomasi, D., & Marinello, F. (2024). Satellite Monitoring of Italian Vineyards and Spatio-Temporal Variability Assessment. *AgriEngineering*, *6*(4), 4107-4134. https://doi.org/10.3390/agriengineering6040232

Zsigmond, T., Bakacsi, Z., & Horel, Á. (2025). Refining grapevine vegetation status by utilizing grassland and remote sensing data. *Scientific Reports*, *15*(1), 31586. https://doi.org/10.1038/s41598-025-16967-6